Available online at www.sciencedirect.com
ScienceDirect
Journal of Power Sources 169 (2007) 117–122
JOURNAL OF POWER SOURCES
www.elsevier.com/locate/jpowsour

Short communication

Hydrogenation properties of pure magnesium and magnesium–aluminium thin films☆

Roger Domènech-Ferrer, Madana Gurusamy Sridharan, Gemma Garcia, Francesc Pi, Javier Rodríguez-Viejo *

Departament de Física, Universitat Autònoma de Barcelona, 08193 Bellaterra, Spain

Available online 30 January 2007

Abstract

We have studied the hydrogenation/dehydrogenation behaviour of multilayered stacks of Pd/Mg/Pd and Pd–Fe(Ti)–Mg–Al–Mg–Fe(Ti)–Pd grown by electron beam physical vapour deposition. The palladium coating was deposited at both sides of the structure to ensure a fast dissociation rate and good transport properties for hydrogen as well as to avoid oxidation of magnesium either from atmosphere as from the substrate surface. Fe and Ti layers were included in the stack composition in order to assess their possible catalyst effect as well as to prevent the formation of Mg_xPd_y intermetallics during the thermal treatments. We have studied the structure evolution after thermal treatments as well as after the hydrogenation and dehydrogenation processes using XRD. We have also followed the reactions kinetics by resistometry and differential scanning calorimetry. The nanostructured Mg films have been hydrogenated at temperature as low as 50 °C in few minutes. Adding aluminium to magnesium has improved its hydrogenation capacity. We have also observed that the formation of an Mg_xAl_y intermetallic before hydrogenation improves the storage capacity. We have confirmed that titanium is a better catalyst for the hydrogenation/dehydrogenation of the Mg films.

Keywords: Magnesium hydrides; Thin films; Hydrogen storage; Mg–Al system

1. Introduction

Metal hydrides represent a promising way of storing hydrogen but major drawbacks due to poor gravimetric efficiency have to be overcome. Among possible candidates, magnesium and magnesium-based alloys are one of the most attractive materials because of their high hydrogen storage capacity (7.6 wt.% for MgH_2), low density and low cost. However, the high enthalpy of formation of MgH_2, responsible for the high-temperature of hydrogen release (552 K at 1 bar), as well as the slow hydriding and dehydriding kinetics difficult its application into real systems [1,2]. A possible solution could come from adding light metal, such as Al or other light group elements. According to Guo and co-workers [3,4] addition of Al to MgH_2 reduces the stability of the hydride leading to an improvement in the dehydrogenation conditions. Moreover, it has also been reported that mixing magnesium with minor amounts of catalytic transition elements, such as Ti or Fe, effectively improves the hydriding and dehydriding kinetics of magnesium at high temperatures [4]. Besides, the addition of light elements may also lead to the formation of complex hydrides, such as $Mg(AlH_4)_2$ with 9.3 wt.% hydrogen storage capacity [5–10].

This paper focuses on the hydrogenation and dehydrogenation behaviour of magnesium and magnesium/aluminium thin films prepared by electron beam evaporation. Thin film preparation would lead to an enhanced control of materials stoichiometry, structural order and grain size. Furthermore, glassy metastable phases with unknown hydrogenation behaviour may be encountered during growth or upon annealing treatments in H_2 atmosphere. In addition, in those systems hydrogenation/dehydrogenation is not kinetically limited lowering the (de)hydrogenation reaction temperatures. X-ray diffraction, differential scanning calorimetry, resistivity and scanning electron microscopy have been used to characterize the structural evolution of the samples before and after the hydrogenation processes

☆ This paper was presented at the 2nd National Congress on Fuel Cells, CONAPPICE 2006, Madrid, Spain, 18–20 October 2006.

* Corresponding author. Tel.: +34 93581 1769; fax: +34 93581215.
E-mail address: javirod@vega.uab.es (J. Rodríguez-Viejo).

0378-7753/$ – see front matter © 2007 Elsevier B.V. All rights reserved.
doi:10.1016/j.jpowsour.2007.01.049

for different aluminium to magnesium ratios. The influence of previous thermal treatments as well as the catalysing effect of Fe and Ti is also described.

2. Experimental

The films were prepared in a Leybold UNIVEX 450 e-beam evaporation set-up at room temperature on both bare and photoresist-coated silicon wafers at room temperature. The evaporation parameters were optimised individually to control the growth rate of the different metals using a quartz microbalance located inside the deposition chamber. Values between 0.1–0.2 nm s^{-1} were used for all the components. When aluminium is added to magnesium, Mg/Al/Mg stacks were sandwiched between Pd/Fe or Ti bilayers at both faces forming a multilayered system: Pd/Fe–Ti/(Mg/Al/Mg)/Fe–Ti/Pd, in order to ensure the correct intimacy of the elements. The Palladium coating of 10 nm was deposited to warrant a fast dissociation rate and good transport properties for hydrogen as well as to avoid oxidation of magnesium either from atmosphere as from the substrate surface. The Fe or Ti layers were deposited in order to assess their possible effect as catalysts of the reaction as well as to prevent the formation of Mg_xPd_y intermetallics during the thermal treatments.

Hydrogenation was typically carried out on as-deposited samples at 150 °C and 1 bar of hydrogen pressure during 1 h. Previously annealed samples were also hydrogenated under the same conditions to study the influence of Mg_xAl_y intermetallic on the hydrogenation properties. Some samples have also been hydrided in a 5% H_2/argon mixture.

Differential scanning calorimetry was performed using a Perkin-Elmer DSC-7, with detection limit of 4 μW. Free-standing films, obtained by dissolving the photoresist resin in acetone, were used to improve the DSC signal-to-noise ratio in comparison with the films on substrates. In order to increase the analysed mass, trimmed portions of the samples were stacked into an aluminium pan for the measurements. For hydrogenation processes realised at 1 bar, aluminium pans containing ∼1 mg sample were heated up to the desired temperature and maintained at this temperature for one hour in a special chamber. Subsequently, the aluminium pan was transferred to the DSC apparatus where the dehydrogenation reactions were studied by heating up the samples at 10 K min^{-1} under a purified flowing Ar atmosphere. In some cases, in situ treatments and measurements of hydrogenation/dehydrogenation in a 5% H_2/Ar atmosphere were also carried out in the DSC system. The large difference in thermal conductivity between the hydrogen that is released in the sample cell with respect to the Ar gas in the reference cell difficults a quantitative determination of the enthalpy of hydrogen desorption. Complementary four-point probe resistivity measurements were performed to detect the resistivity changes expected from the formation or decomposition of hydride phases. Before those measurements the chamber was purged three times with Nitrogen and evacuated to 10^{-3} Torr. A blank test on samples only heated in vacuum to 150 °C was conducted before each hydrogenation. The morphology of the films was studied by scanning electron microscopy with a JEOL JSM-6300 microscope before and after treatments.

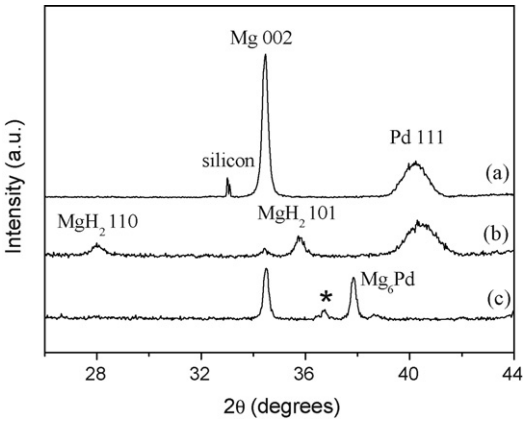

Fig. 1. XRD patterns of 300 nm thick Mg layers (a) as-prepared, (b) after hydrogenation treatment at 150 °C during 4 h in 1.0 bar of pure H_2 and (c) after dehydrogenation process annealing up to 350 °C with a heating rate of 10 K/min.

3. Results and discussion

3.1. Pure Mg films

In order to study the hydrogenation of pure magnesium films we prepare 50–300 nm thick films embedded in 10 nm of Pd onto resin coated silicon substrates. Fig. 1 shows the XRD pattern of the thin film sample in the as-deposited state (a), after hydrogenation at 150 °C in pure H_2 (b) and after a thermal treatment up to 250 °C in Ar. In the as-deposited state only reflections corresponding to the Mg and Pd were observed along with a small signal of the silicon substrate. We notice that only the 0 0 0 2 reflection of the Mg was observed confirming the 0 0 0 *l* preferred orientation of the layers. Using the Scherrer formula we estimate the grain size of our magnesium layers between 30 and 180 nm for thinner and thicker films, respectively. Upon hydrogenation reflections corresponding to MgH_2 clearly appear but still some Mg traces are detected. After the dehydrogenation process no signal of MgH_2 was detected and large amount of Mg reappears along with the Mg_6Pd intermetallic that has been formed due to the high temperature attained during the dehydrogenation process. It is important to notice that the complete disappearance of the Mg peak as a consequence of the H_2 treatment is not a guarantee of full theoretical hydrogenation (7.6 wt.% H_2) as has been already stated by other authors [11].

The electrical characterisation of magnesium samples was performed from room temperature to 150 °C in pure H_2 atmosphere for hydrogenation (Fig. 2(a)) followed by a heating up in vacuum for dehydrogenation (Fig. 2(b)). Upon exposure to hydrogen the thin Mg film resistance increases sharply from values as low as 50 °C. These changes in the electrical properties are related to a metallic to a semi-insulating state transition, which corresponds to a phase change from Mg to MgH_2. Dehydrogenation was also tested under dynamic heating. On the contrary to the former case, resistance decreases considerably upon heating. Fig. 2(b) shows that H_2 desorption starts around 130 °C

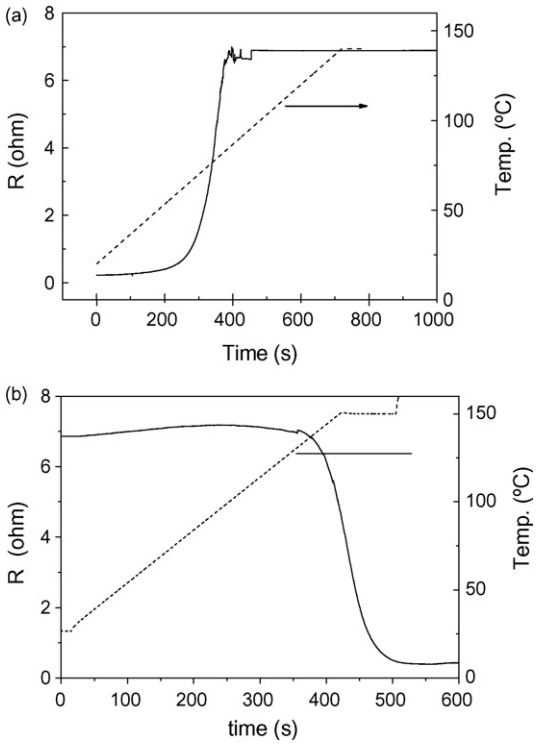

Fig. 2. Resistivity measurement heating up the sample from room temperature to 140 °C in (a) hydrogen atmosphere and (b) vacuum atmosphere.

and evolves during the isothermal annealing at 140 °C reaching similar resistance values as the as-deposited metallic sample within 100 s. This is due to the removal of hydrogen from the magnesium hydride phase formed during hydrogenation. The dehydrogenation temperature was lowered to avoid the formation of Mg_6Pd alloy. The enhanced kinetics, compared to bulk samples [1], of the hydrogenation/dehydrogenation process is related to the nanocrystalline nature of the samples, i.e. diffusion of H_2 through MgH_2 is not a rate limiting step. Nevertheless, we have to mention that no remarkable differences in the hydrogenation/dehydrogenation temperatures were detected as a function of grain size at least for the studied Mg film thicknesses.

In situ hydrogenation (heating to 160 °C in 5% H_2/Ar) /dehydrogenation (heating to 210 °C in pure Ar) experiments were also performed within the DSC using samples detached from the silicon substrate as described in Section 2. Fig. 3 shows the results after three consecutive dehydrogenation cycles. In the three cases, we can observe the endothermic reaction assigned to the dehydrogenation process. The desorption temperature slightly above 140 °C closely agrees with the value extracted from the resistivity measurements for samples hydrided in 1 atm of pure H_2. We can also observe that during cycling there is a decrease of the hydrogen content, as the area of the measured peak is significantly reduced. This phenomenon could be due to magnesium oxidation along the cracks formed during previous cycling. The inset in Fig. 3 shows the DSC trace of a commercial MgH_2 powder where the desorprtion at the same experimental conditions started around 440 °C. The slower kinetics of dehydrogenation compared to the nanocrystalline thin films is clearly identified by the higher desorption temperature.

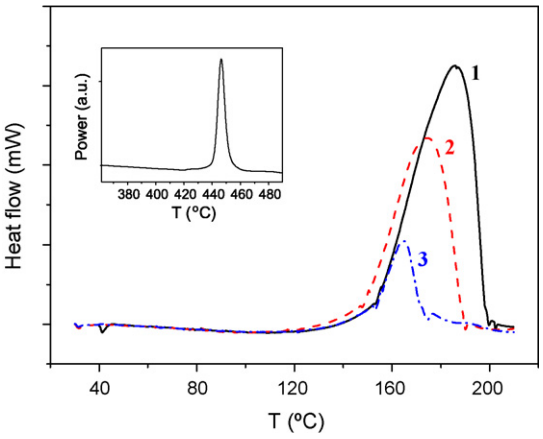

Fig. 3. DSC traces showing the dehydrogenation behaviour of 300 nm thick Mg layers covered by 10 nm Pd during cycling. Inset shows the DSC dehydrogenation curve of commercial MgH_2.

3.2. Mg–Al films

As we have seen in Fig. 1, some traces of Mg are still present after the hydrogenation process. In order to increase the performance of the system and thus be able to hydride larger quantities of magnesium we analyze the influence of aluminium in magnesium samples. As described in the introduction, aluminium can also improve the thermodynamics of the desorption process [2,3].

Different Al/Mg ratio were studied by preparing multilayers of Mg/Al/Mg varying the thickness of both aluminium and magnesium layers. A poor magnesium sample (38.5 at%) was prepared by sandwiching 127 nm of aluminium between two 55 nm thick Mg layers, a 56 at% sample was prepared with 127 nm Al and two 115 nm Mg layers, and a rich magnesium layer was obtained with only 4 nm of aluminium separating two 115 nm magnesium layers. As-deposited samples, as well as after thermal treatments of hydrogenation and/or dehydrogenation were characterized by XRD (Fig. 4). In the as-deposited films, only the reflections corresponding to the pure elements were detected. The Mg layer grows with a strong preferred orientation along the [0 0 0 2] direction as already mentioned. Ten nanometers of iron were added between Pd and Mg to avoid the possible formation of intermetallics. Because of the nanometric thickness of the palladium and iron layers the corresponding XRD peaks were rather wide.

After annealing at 150 °C in vacuum, the Mg_2Al_3 ($2\theta = 36.37°$) was generally observed except in the 98% at sample, where the ratio of aluminium was to poor to give rise to the alloy formation. For the same reason in the 56% samples some traces of free magnesium are also detected. In the rich aluminium samples, the Al 1 1 1 reflection completely vanishes after thermal treatment. For the 98% Mg sample aluminium was not directly identified by XRD, but after the thermal treatment the Mg 0 0 0 2 peak shifted to higher angles probably because of the formation of an (Al)Mg solid solution. Previously annealed samples were hydrogenated in 1 bar H_2 at 150 °C during 1 h. The XRD patterns display some differences as a function of the aluminium content. As expected the Mg_2Al_3 was converted into MgH_2 and Al fol-

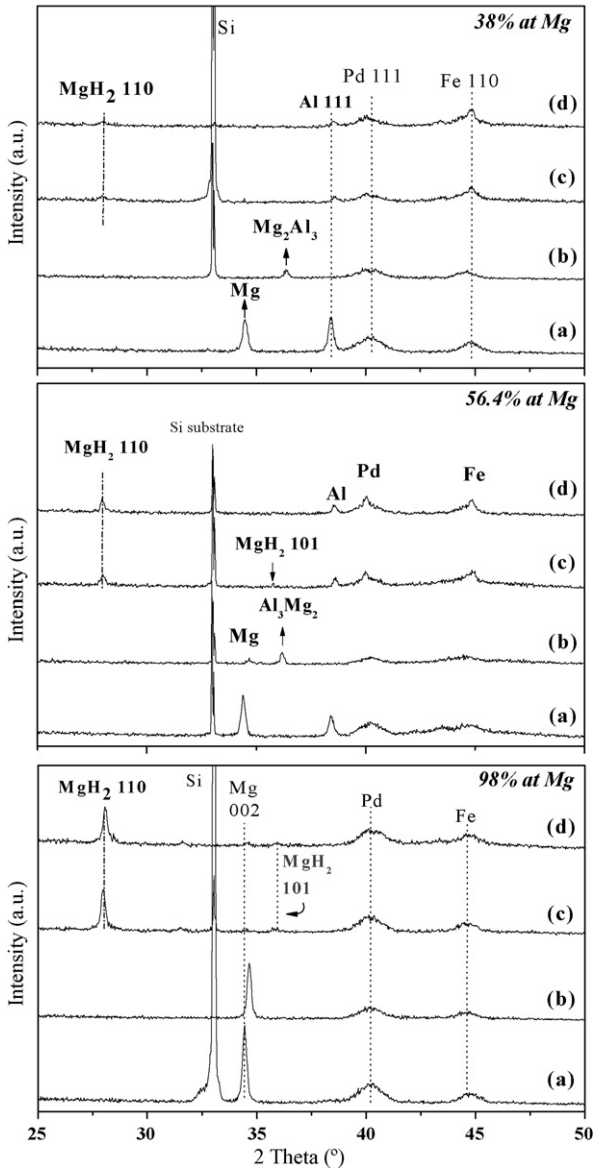

Fig. 4. XRD pattern of Mg–Al samples varying the Al contain from 38, 56.4 and 98 at% Mg in the (a) as-deposited; (b) after thermal treatment at 250 °C during 1 h in vacuum; (c) b samples hydrogenated at 150 °C during 1 h in 1 bar of pure H_2; (d) c samples dehydrogenated at 120 °C during 1 h in vacuum.

lowing the reaction: $Mg_2Al_3 + 2H_2 \rightleftarrows 2MgH_2 + 3Al$, and in the 98 at%. Mg along with the MgH_2 we still detected traces of non hydrided Mg.

It is worth noting that if we compare samples with 38 and 56.4 with those with 98% at Mg, we can see the positive effect of adding aluminium to magnesium. Specially, if we compare 56.4 with 98% samples, where the total magnesium thickness was 250 nm in both cases, but separated by 127 or 4 nm of aluminium, respectively, we can see that in the first case magnesium is completely hydrogenated. The aluminium layer seems thus to act as an activator for the hydrogenation reaction. On the contrary, we did not desorb hydrogen from the samples at 120 °C, which shows that the addition of aluminium did not significantly improve the desorption temperature compared to pure Mg films, with a desorption temperature around 130–140 °C. These results will be further discussed below.

In order to still improve the stack composition we have tested the influence of Ti on the hydrogenation/dehydrogenation behaviour of the Mg–Al samples. We prepared by e-beam magnesium and aluminium thin films with the following structure: 10 nm Pd/10 nm Fe or Ti/50 nm Mg/143 nm Al/50 nm Mg/10 nm Fe or Ti/10 nm Pd. Those thickness were selected to prepare samples with a composition around the 33% at of magnesium which is close to $Mg(AlH_4)_2$ alanate. The as-prepared samples followed different treatments: hydrogenation in pure hydrogen and in a 5% hydrogen–argon mixture. Even that in the former study we have seen that the magnesium hydride could be formed from the intermetallic Mg_xAl_y phase, the hydride peak intensities were rather weak, and it is expected that a direct hydrogenation of the pure metals may result in an enhanced behaviour. XRD was used to determine the structural evolution of the samples as shown in Fig. 5.

In both cases as-deposited samples (a) only showed the reflections corresponding to the Mg, Al, Pd and Fe or Ti depending on the library. We have to notice that the Al 1 1 1 and Ti 1 1 0 peaks are superposed and very difficult to be distinguished. In the thermal treated samples (b), the reflections assigned to Mg and Al vanished and the reflections clearly assigned to Mg_2Al_3

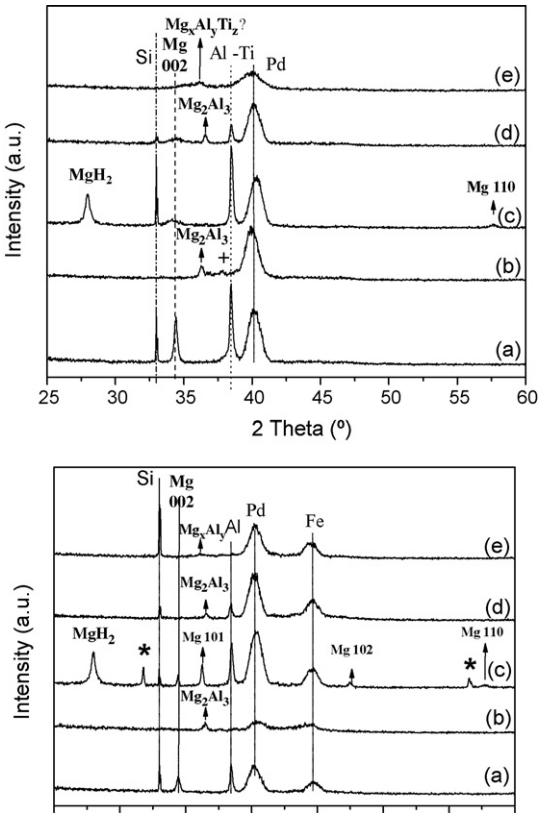

Fig. 5. XRD patterns of Mg–Al samples with 33 at% Mg adding Ti or Fe (a) in the as-deposited state; (b) after thermal treatment 250 °C during 1 h in vacuum, (c) a samples hydrogenated at 150 °C during 1 h in 1 bar of pure H_2; (d) a samples hydrogenated at 150 °C in 5% H_2–Ar mixture during 1 h; (e) c samples dehydrogenated at 190 °C during 20 min in vacuum.

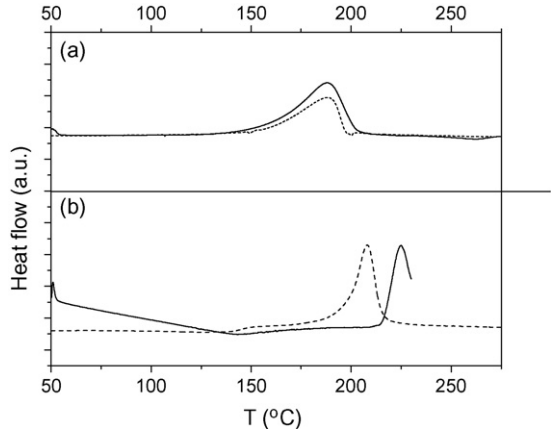

Fig. 6. (a) Calorimetric traces of the dehydrogenation behaviour of Pd/Mg/Pd and Pd/Fe/Mg–Al/Fe/Pd films (continous line) in Ar atmosphere and (b) DSC comparison between Pd/Fe/Mg/Fe/Pd films (continous line) and Pd/Ti/Mg–Al/Ti/Pd (dashed line) during dehydrogenation in a 5% H_2/Ar atmosphere.

appeared. In the case of Ti doped samples, an unassigned reflection was also observed around 38°, we believe that it can be related to the presence a solid solution formed by $Mg_xAl_yTi_z$. In the samples hydrogenated at 150 °C in pure H_2 (Fig. 5c), the results were quite different from one sample to the other. In the case of samples with Fe, along the Pd and Fe reflections and some traces of Mg 0 0 0 2, 1 0 1 1, 1 0 1 2 and Al 1 1 1, we detect the appearance of MgH_2. Nevertheless, we have also observed two other peaks marked with an asterisk (*) at 31.8° and 56.5° that have not been unambiguously assigned yet, but that may correspond to a new hydride phase. It is tempting to relate this phase to Mg alanate, ($Mg(AlH_4)_2$) [PDF 470980], as angle reflections corresponded and as we are working with samples with 33 at%. Mg approximately, which is close to the expected Mg/Al atomic ratio in this complex hydride. On the contrary, hydrogenated Ti samples only show the MgH_2 peak and high intensity of Ti/Al and Pd reflections. Very small traces of Mg 0 0 0 2 and 1 1 2 0 still coexist with the hydride. Samples hydrogenated with 5% H_2/Ar showed different behaviour, no MgH_2 was detected in any sample but the signal of Mg vanished and the Al (Al/Ti) diminishes to form intermetallic compounds. Although we did not detect crystallized MgH_2 its presence has been demonstrated by calorimetric experiments, as will be discussed below (see Fig. 6). Fig. 5(e) corresponds to the samples shown in Fig. 5(c) after dehydrogenation at 190 °C during 20 min in vacuum. The MgH_2 peak vanishes, however no recovery of the Mg 0 0 0 2 line is seen, which may be attributed to the nanocrystallization process that occurs due to volume differences between Mg and MgH_2. The Al or Al/Ti signal also vanishes and thus the peak corresponding to the intermetallic shifted to low angles, especially in the case of Ti samples new glassy alloys has been formed with Mg, Al and Ti.

Fig. 6(a) shows a comparison of the dehydrogenation behaviour between a pure Pd/Mg/Pd film and a Pd/Fe/Mg–Al/Fe/Pd (33 at% Mg) film after being submitted to hydrogenation at 150 °C for 1 h in 1 bar of H_2. Both samples show a similar behaviour which clearly indicates neither the Fe layer nor the presence of Al seems to improve the dehydrogenation behaviour of the films.

Comparing results from Figs. 4 and 5, it turns clear that hydrogenating the samples forming previously the alloys as an intermediate step give rise to apparently better hydrogenated samples as almost no trace of free magnesium persist after the hydrogenation treatment while hydriding from the as-deposited state give rise to magnesium hydride mixed with alloys and traces of pure Mg. We can also mention that in the hydrogenated samples from the as-deposited state, the magnesium grains lost their preferential 0 0 0 2 orientation as we detect Mg 0 0 0 2 and 1 0 1 2 reflections. The direct hydrogenation process seems to be accompanied by a nanocrystallization process in the Mg films.

From Fig. 5, we can also see that after treatment in pure H_2 the amount of non hydrogenated Mg is lower in the case of Ti doped samples than in the Fe samples, confirming the catalyser effect of Ti. The improved desorption temperature (T = 195 °C) of the Ti-doped sample with respect to pure Mg (215 °C) estimated from the thermograms obtained in a 5% H_2/Ar atmosphere (Fig. 6(b)) assess the catalytic effect of the thin Ti films. In Fig. 6(b), we can observe both the exothermic and endothermic features related to absorption and desorption of hydrogen, respectively. As the whole thermogram is registered in a reduced hydrogen pressure the onset temperatures for hydrogen release and absorption are higher than those measured in pure Ar or hydrogen, respectively.

Images of the surface morphology obtained by SEM of the Ti doped hydrogenated sample confirmed the higher hydrogenation of those films. It is well known that Mg tends to disintegrate due to volume expansion upon hydrogenation. In the case of Mg thin films; this phenomenon is accompanied by the formation of

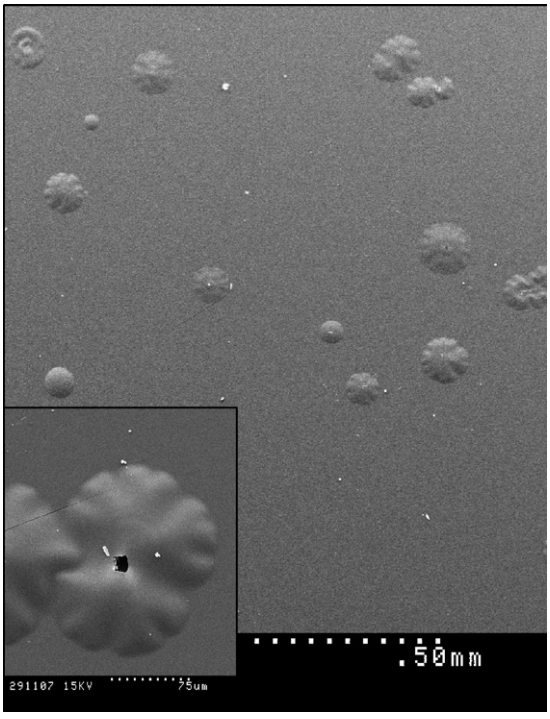

Fig. 7. SEM micrographs of the surface morphology of 33 at%. Mg sample doped with titanium after the dehydrogenation process (Fig. 5e). Inset shows a detail of the produced bubbles.

cracks and detachment of the layers because of the build up of compressive stresses during the hydrogenation process. As can be seen in Fig. 7, Ti doped samples after hydrogenation, showed peeling-off that are not present in the as-deposited state neither in the Fe hydrogenated samples. In that case, the peeling has a bubble form that has already been observed by Pranevicius and Milcius [5,6]. They assess that this morphology comes from the hydrogen release in the MgH_2 layers. In our case, the density of buckled regions increases during the hydrogenation treatment. The dehydrogenation process releases the stress of the layers and the surface flattens again.

4. Conclusions

This study shows that Pd/Mg/Pd and Pd/(Fe, Ti)/Mg–Al/(Fe, Ti)/Pd thin films absorb hydrogen at low temperatures and 1 atm H_2 with excellent kinetics. The Al addition has a beneficial effect on the hydrogenation characteristics of the Mg films, without a significant difference in the desorption temperature. Samples with a Fe overlayer and a Mg content around 33% at showed the presence of additional X-ray peaks which match those of a complex hydride with an alanate structure. The incorporation of Ti enhances the hydrogenation of the films at the expense of inducing their partial detachment from the substrate after hydrogenation. The addition of a Ti thin film also lowers the onset of temperature for dehydrogenation compared to Pd/Mg/Pd and Pd/Fe/Mg–Al/Fe/Pd films, confirming the catalysing effect of Ti.

Acknowledgements

The authors acknowledge financial support from Air Products and Chemicals, MATGAS 2000 AIE and from the Dirección General de Investigación and Direcció General de Recerca under Projects MAT2004-04761 and 2005SGR00201, respectively. We also thank the Servei de Microscopia of UAB.

References

[1] J.L. Bobet, C. Even, Y. Nakamura, E. Akiba, B. Darriet, J. Alloys Compd. 298 (2000) 279.
[2] K.H.J. Buschow, P.C.P. Bouten, A.R. Miedem, Rep. Progr. Phys. 45 (1982) 937.
[3] Y. Song, Z.X. Guo, R. Yang, Phys. Rev. B 69 (2004) 094205.
[4] C.X. Shang, M. Bouodina, Y. Song, Z.X. Guo, Int. J. Hydrogen Energy 29 (2004) 73–80.
[5] L.L. Pranevicius, D. Milcius, Thin Solid Films 483 (2005) 135–140.
[6] L.L. Pranevicius, D. Milcius, J. Alloys Compd. 373 (2004) 9–15.
[7] R. Gremaud, A. Borgschulte, C. Chacon, J.L.M. Van Mechelen, H. Schereuders, A. Züttel, B. Hjörvarsson, B. Dam, R. Griessen, Appl. Phys. A 84 (2006) 77–85.
[8] R. Gremaud, A. Borgschulte, H. Schereuders, A. Züttel, B. Dam, R. Griessen, J. Alloys Compd. 404–406 (2005) 775–778.
[9] Z.F. Hou, J. Power Sources 159 (2006) 111–115.
[10] M.J. Van Setten, G.A. de Wijs, V.A. Popa, G. Brocks, Phys. Rev. B 72 (2005) 073107.
[11] K. Higuchi, H. Kajioka, K. Toiyama, H. Fujii, S. Orimo, Y. Kikuchi, J. Alloys Compd. 293–295 (1999) 484–489.